and its error becomes

$$\phi_\varepsilon = \frac{5ab}{5544}\lambda^{11} = \frac{ab}{54,140,625,000}(\Omega T)^{11} \tag{27}$$

Algorithm 4 (Six Samples)

The six-sample algorithm has not been previously introduced. However, using the proposed method it can be easily accomplished. In this case $n = 6$, $p = 0$, and $N = 6$, and k_i can be calculated from Eq. (17) as follows:

$$k_1 = \frac{15,797}{4620}, \qquad k_2 = \frac{3917}{2310}, \qquad k_3 = \frac{608}{385}$$
$$k_4 = \frac{2279}{2310}, \qquad k_5 = \frac{463}{924} \tag{28}$$

Hence, the algorithm becomes

$$\delta\hat{\phi}_m = [k_5\Delta\boldsymbol{\theta}_m(1) + k_4\Delta\boldsymbol{\theta}_m(2) + k_3\Delta\boldsymbol{\theta}_m(3) + k_2\Delta\boldsymbol{\theta}_m(4) + k_1\Delta\boldsymbol{\theta}_m(5)] \times \Delta\boldsymbol{\theta}_m(6) \tag{29}$$

Its error can also be calculated from Eq. (21), and it becomes

$$\phi_\varepsilon = \frac{ab}{4004}\lambda^{13} = \frac{ab}{52,295,018,840,064}(\Omega T)^{13} \tag{30}$$

The error for six-sample algorithm has the 13th power of ΩT, and it concurs with the earlier statement that the magnitude of error depends mainly on the total number of samples.

Conclusion

In this Note, a formalized approach to obtaining optimal coefficients for strapdown coning compensation algorithms is proposed. It is shown by examples that optimal coefficients for the existing attitude algorithms and the six-data interval case can easily be obtained using the proposed approach. The main advantage of using the formalized approach is its easy applications to various combinations of sample numbers. Thus, it enables the attitude algorithm designers to choose the most effective coning compensation algorithm for their attitude computation specifications efficiently.

Acknowledgment

This work was supported by the Special Project Fund given to the Automatic Control Research Center, Seoul National University, by the Agency for Defense Development.

References

[1]Wilcox, J. C., "A New Algorithm for Strapdown Inertial Navigation," *IEEE Transactions on Aerospace and Electronic Systems*, Vol. AES-3, No. 5, 1967, pp. 796–802.

[2]Bortz, J. E., "A New Mathematical Formulation for Strapdown Inertial Navigation," *IEEE Transactions on Aerospace and Electronic Systems*, Vol. AES-7, No. 1, 1971 , pp. 61–66.

[3]Jordan, J. W., "An Accurate Strapdown Direction Cosine Algorithm," NASA TN D-5384, Sept. 1969.

[4]Miller, R. B., "A New Strapdown Attitude Algorithm," *Journal of Guidance, Control, and Dynamics*, Vol. 6, No. 4, 1983, pp. 287–291.

[5]Ignagni, M. B., "Optimal Strapdown Attitude Integration Algorithms," *Journal of Guidance, Control, and Dynamics*, Vol. 13, No. 4, 1990, pp. 738–743.

[6]Lee, J. G., Yoon, Y. J., Mark, J. G., and Tazartes, D. A., "Extension of Strapdown Attitude Algorithm for High-Frequency Base Motion," *Journal of Guidance, Control, and Dynamics*, Vol. 13, No. 4, 1990, pp. 738–743.

[7]Jiang, Y. F., and Lin, Y. P., "Improved Strapdown Coning Algorithms," *IEEE Transactions on Aerospace and Electronic Systems*, Vol. AES-28, No. 2, 1992, pp. 484–490.

[8]Ignagni, M. B., "Efficient Class of Optimal Coning Compensation Algorithms," *Journal of Guidance, Control, and Dynamics*, Vol. 19, No. 2, 1996, pp. 424–429.

[9]Jiang, Y. F., and Lin, Y. P., "On the Rotation Vector Differential Equation," *IEEE Transactions on Aerospace and Electronic Systems*, Vol. AES-27, No. 1, 1991, pp. 181–183.

[10]Savage, P. G., "Strapdown System Algorithms," AGARD-LS-133, 1984, pp. 202–212.

Flutter Boundary Prediction Using Physical Models and Experimental Data

A. Turevskiy,* E. Feron,† and J. Paduano‡
Massachusetts Institute of Technology, Cambridge, Massachusetts 02139

I. Introduction

THE possible occurence of flutter is an important factor that slows down the aircraft flight envelope clearance because it is not very well known in advance and might have catastrophic consequences. Any improvement in predicting the aircraft flutter boundary might, therefore, simultaneously impact the safety and cost of the flight test process.[1]

Several techniques exist to predict flutter boundaries. The first is to track the damping ratios of all flexible modes of the aircraft[2]: Proximity to flutter is declared when one or more damping ratios are approaching zero. Accurate flutter boundary predictions based on this approach require the aircraft to be very close to the actual flutter boundary. This method is nevertheless very popular because it is computationally inexpensive.

Another way to predict the flutter boundary is to develop and use analytical models of aircraft flexible dynamics and unsteady aerodynamic forces. The structural part of the model is obtained from finite element analysis, whereas unsteady aerodynamic forces are approximated using standard linear systems theory.[3,4] In this model, dynamic pressure and Mach numbers are parameters that may be varied until the model dynamics are unstable, thus providing an analytical flutter boundary estimate. From that standpoint, it is similar to the so-called p–k iteration method.[5] This approach provides a priori information about possible flutter mechanisms and flutter boundaries. The quality of the results remains, however, dependent on modeling accuracy.

In this Note, a simple method is developed to update a physical aircraft wing mathematical model with wind-tunnel test data to predict more reliable flutter boundary estimates. The method could potentially apply to full aircraft models and flight test data as well. It uses nonlinear optimization to match the poles of the analytical model to the experimentally identified poles of the aircraft. From that standpoint, the proposed method is similar, but not identical to previous research efforts.[6,7] It is experimentally validated on a wind-tunnel entry.

II. Models and Data for Flutter Boundary Estimation

Analytical Models

A common aircraft aeroelastic model is written in the Laplace transform domain as[4]

$$Ms^2\eta(s) + Cs\eta(s) + K\eta(s) + \bar{q}Q(s)\eta(s) = 0 \tag{1}$$

The first three terms M, C, and K correspond to the system's mass, damping, and stiffness matrices, respectively. The fourth term represents the effect of aerodynamics on the system, and $\bar{q} = \rho V^2/2$ is the dynamic pressure. The effect of unsteady aerodynamics is captured by rational functions of the form

$$Q(s) = A_0 + A_1\bar{s} + A_2\bar{s}^2 + [\bar{s}/(\bar{s} + \beta_1)A_3] + [\bar{s}/(\bar{s} + \beta_2)A_4] \quad \text{with} \quad \bar{s} = (b/V)s$$

Received June 4, 1998; revision received Sept. 5, 1998; accepted for publication Sept. 8, 1998.

*Graduate Research Assistant, Department of Aeronautics and Astronautics, 77 Massachusetts Avenue; currently Engineer, Propulsion Systems Analysis Department, Pratt and Whitney. E-mail: turevska@pweh.com.

†Assistant Professor, Department of Aeronautics and Astronautics, Room 33-217, 77 Massachusetts Avenue. E-mail: feron@mit.edu. Senior Member AIAA.

‡Associate Professor, Department of Aeronautics and Astronautics, Room 33-103, 77 Massachusetts Avenue. E-mail: jdpaduan@mit.edu. Member AIAA.

where A_0, A_1, A_2, A_3, and A_4 are matrix coefficients to be determined and b is a normalizing constant (often chosen to be the semichord). Introducing the reduced parameters

$$\tilde{K} = K + \bar{q}A_0, \qquad \tilde{C} = C + \bar{q}(b/V)A_1$$
$$\tilde{M} = M + \bar{q}(b/V)^2 A_2 \tag{2}$$

Eq. (1) can be written in state-space form as

$$\begin{bmatrix} \dot{\eta} \\ \ddot{\eta} \\ \dot{x}_1 \\ \dot{x}_2 \end{bmatrix} = A(\bar{q}, V) \begin{bmatrix} \eta \\ \dot{\eta} \\ x_1 \\ x_2 \end{bmatrix}$$

with

$$A(\bar{q}, V) = \begin{bmatrix} 0 & I & 0 & 0 \\ -\tilde{M}^{-1}\tilde{K} & -\tilde{M}^{-1}\tilde{C} & -\bar{q}\tilde{M}^{-1}A_3 & -\bar{q}\tilde{M}^{-1}A_4 \\ 0 & I & -(V/b)\beta_1 I & 0 \\ 0 & I & 0 & -(V/b)\beta_2 I \end{bmatrix}$$

This dynamical model is restricted to capture flutter phenomena based on linear effects.

In-Flight Measurements

Experimental measurements are obtained when the aircraft is on the ground (ground tests) and at several operating points during the wind-tunnel experiment (or flight test). These measurements may be obtained using excitation and sensing devices. Assuming a linear response of the system, the flight test data may then be condensed into transfer functions[8] and modal information (natural frequencies and damping) can then be extracted.

III. Predicting Flutter Boundaries

The proposed approach to perform flutter boundary prediction is to match the available physical model with the experimental data as they are collected. Matching an analytical model of aircraft behavior to experimental data may be seen as an identification problem. Such a task involves the definition of the appropriate decision variables, a metric, and an optimization algorithm. The approach is similar to optimization-based approaches to fit a rational approximation of the wing or aircraft aeroelastic behavior to computer-generated unsteady aerodynamic force coefficients.[9]

Optimization Parameters

The most important parameters affecting the system are K, C, and M and the aerodynamic coefficients A_0, A_1, A_2, A_3, and A_4. The structural coefficients K, C, and M are usually adjusted at zero dynamic pressure, using static and dynamic ground test data. Because this phase is less critical both in terms of cost and safety than the flight test itself, it will be assumed that the model in Eq. (1) is already tuned to ground test data. The aerodynamic coefficients A_0, A_1, A_2, A_3, and A_4 are then used to adjust the physical model to in-flight data. A subset of these matrices may be chosen to be the decision variables, by selecting only those modes that are deemed critical to the flutter inception process. The coefficients β_1 and β_2 are set to default values.[4]

Performance Metric

The proposed cost function J measures the discrepancy between the natural frequencies and dampings provided by the model and those provided by experimental data at different flight conditions and is written

$$J(A) = \sum_{l=1}^{L} \sum_{k=1}^{K} | \lambda_k[A(\bar{q}_l, V_l)] - \bar{\lambda}_k(\bar{q}_l, V_l)| \tag{3}$$

where $\lambda_k[A(\bar{q}_l, V_l)]$ [respectively $\bar{\lambda}_k(\bar{q}_l, V_l)$] is the analytical (respectively experimental) kth eigenvalue (corresponding to a flexible mode) of the system at the operational condition $(\bar{q}_l, V_l)$. It was found that good estimates of modal frequencies and dampings could be obtained by fitting rational transfer functions to the available experimental transfer functions, using the routine FITMAG found in MATLAB's μ-Analysis and Synthesis Toolbox.[10]

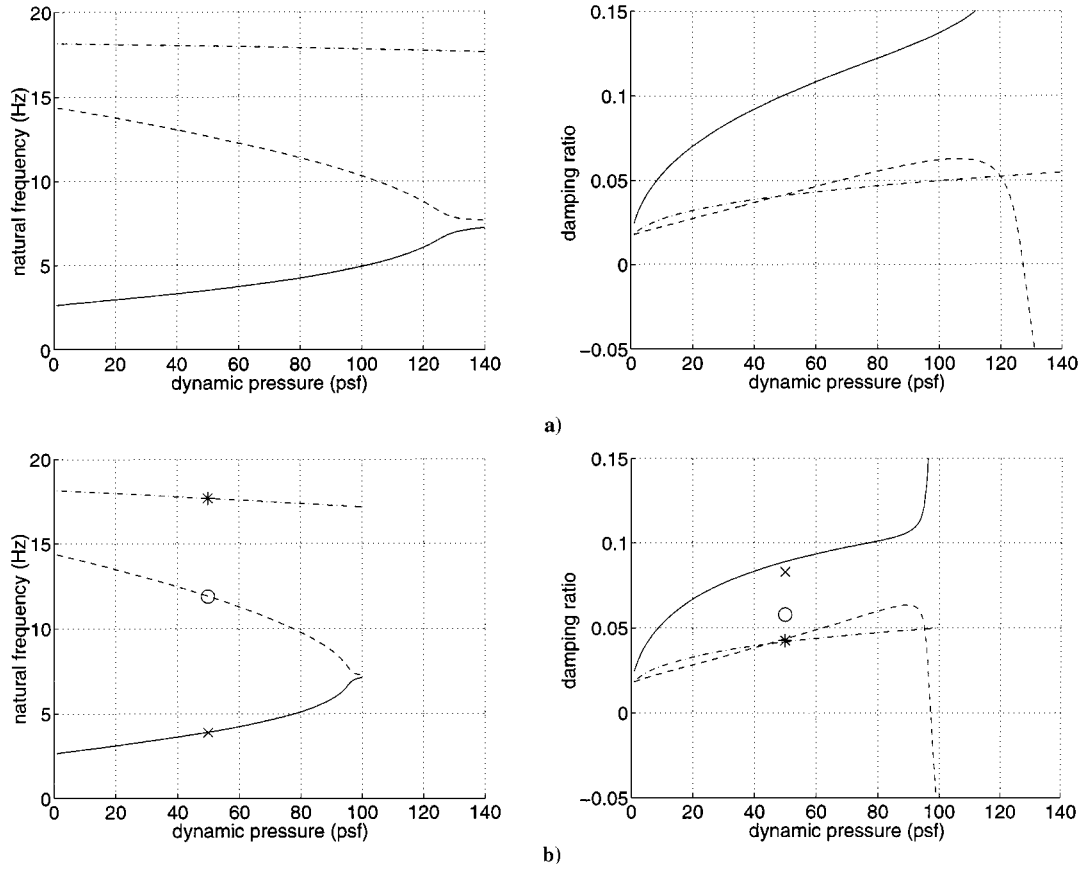

Fig. 1 Evolution of flutter boundary estimates; mode 1: ——, predicted, ×, experimental; mode 2: - - - -, predicted, ∘, experimental; mode 3: – · –, predicted, ∗, experimental; a) no flight data and b) data at 50 psf.

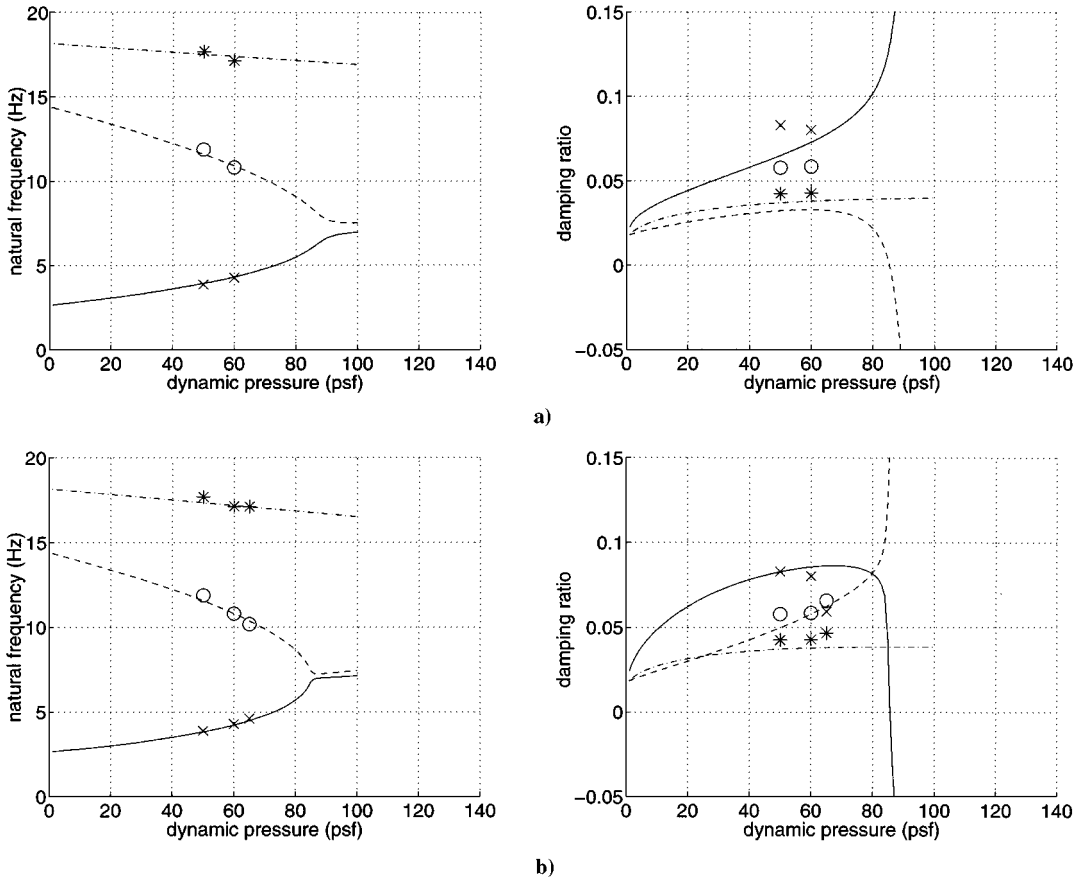

Fig. 2 Evolution of flutter boundary estimates; mode 1: ——, predicted, ×, experimental; mode 2: - - - -, predicted, ∘, experimental; mode 3: – · –, predicted, ∗, experimental; a) data at 50 and 60 psf and b) data at 50, 60, and 65 psf.

Numerical Optimization

Minimizing $J(A)$ over the parameters A_0, A_1, A_2, A_3, and A_4 may be done using a Broyden-Fletcher-Goldfarb-Shanno quasi-Newton optimization method.[11] This is a highly nonlinear and nonconvex optimization problem, and local minima may be encountered. Once a stationary solution is found, the identified model can be used for the flutter boundary prediction. The smallest value of dynamic pressure $\bar{q}$ that makes the system unstable can be found using binary search.[§]

IV. Experimental Validation

Experimental System

The wind-tunnel experiment is a clamped wing.[3,12] Although it does not capture all of the flutter modes that may arise in an aircraft (especially those involving fuselage/wing or tail/wing interactions), opening its flight envelope already appears to be a time-consuming and difficult task.[3] Besides, the experiment was very well archived and documented and was driven very close to the flutter boundary, which is not encountered often on purpose with full-size experimental aircraft. The wing was originally constructed as a testbed for active flutter control. To provide either excitation or control signals, 15 piezoelectric actuators were used. The sensor setup included 10 strain gauges and 4 accelerometers.[12]

Available Models and Data

A physical model was developed[3] to accurately capture the dynamics of the wing. Preliminary analysis determined that only the first three flexible modes were significant in the flutter inception mechanism, and a corresponding reduced model was developed and is given in the Appendix. This model was tuned to match the measured frequencies and dampings during ground vibration tests.[3]

The wing was tested in the wind tunnel to determine the flutter boundary experimentally. Significant input/output data and reliable transfer functions were collected at 50, 60, 65, 70, and 75 psf (corresponding to 204.98, 224.54, 233.71, 242.53, and 251.05 ft/s, respectively). The wing was cleared up to 80.2 psf (259.6 ft/s), very close to the actual flutter speed, which was determined to be 82 psf (262.5 ft/s) via linear extrapolation of the evolution of the damping ratio. Table 1 contains the averages of the estimates of natural frequencies w_i and damping ratios g_i of the first three structural modes.

Table 1 Estimates of natural frequencies and damping ratios from the experimental data

Dynamic pressure $\bar{q}$, psf	Natural frequency		Damping ratio	
50	w_1	3.8673	g_1	0.0829
	w_2	11.8748	g_2	0.0577
	w_3	17.6739	g_3	0.0424
60	w_1	4.2784	g_1	0.0802
	w_2	10.8004	g_2	0.0584
	w_3	17.1191	g_3	0.0428
65	w_1	4.5968	g_1	0.0592
	w_2	10.1733	g_2	0.0656
	w_3	17.1040	g_3	0.0465

Model Fit and Flutter Boundary Prediction

Four models were used to compute the flutter boundary: using the original physical model; then the model fit with data obtained at 50 psf only; then using the data available at 50 and 60 psf only, concluding with the data taken at 50, 60, and 65 psf. The predicted flutter boundaries were 127, 97.2, 85.3, and 85.1 psf, respectively. Therefore, the predicted flutter boundary gets more accurate as more data is used to update the physical model. Figures 1 and 2 show the locus of natural frequencies and damping ratios of the first three structural modes with change in dynamic pressure for the four flutter boundary predictions. According to the experimental data taken very close to flutter, the flutter mechanism of the wing is the coupling of

[§]A file implementing the optimization procedure is available via anonymous FTP from merlot.mit.edu in the directory /pub/feron/flutter_prediction.

the first (bending) and second (torsion) structural modes, with the bending mode going unstable. The initial physical model predicts that it is the second mode that goes unstable. However, when this model is tuned using experimental data available at 50, 60, and 65 psf, the correct flutter mechanism is then predicted. Although the damping ratio of the first mode dips sharply at 65 psf and seems to indicate flutter to occur at 70 psf, the proposed approach still predicts the correct flutter boundary. This shows the interest of relying both on experimental data and also physically significant models.

V. Conclusion

A simple method for flight flutter clearance is presented. This method uses both an analytical model of the flexible dynamics of the wing (or aircraft) and wind-tunnel (or in-flight) experimental data. The advantage of this method in comparison to traditional flight flutter clearance methods is its ability to produce reliable flutter boundary estimates using the experimental data obtained in flight conditions still far away from flutter. The proposed method is validated on a wind-tunnel experiment. The results show that the method can considerably improve the flutter boundary estimates compared with predictions provided by an analytical model alone. An operational implementation of the proposed flutter prediction procedure would require significantly more work, including the automation of many of the aforementioned steps.

Appendix: Physical Models

The mass matrix M is normalized to be the identity. The stiffness matrix K and damping matrix D are 3 by 3 and diagonal, with the following diagonal elements:

$$K = \text{diag}[277.237 \quad 8266.0 \quad 13250.0]$$
$$C = \text{diag}[0.402940 \quad 2.909361 \quad 2.923759] \tag{A1}$$

The lag poles are $\beta_1 = 0.187999$ and $\beta_2 = 4.096000$. The normalizing constant is $b = 6.75$ in. and density $\rho = 1.1478.10^{-7}\text{lb} \cdot \text{s}^2/\text{in.}^4$. The initial aerodynamic matrices estimates are also 3 by 3 and are given by

$$A_0 = \begin{bmatrix} -467.39 & -836.00 & 144.10 \\ 3397.00 & 5760.00 & -758.00 \\ 1467.00 & 4004.00 & 531.80 \end{bmatrix}$$

$$A_1 = \begin{bmatrix} -6391.50 & -5789.52 & 5959.07 \\ 3948.12 & -4559.45 & -844.78 \\ 10946.81 & 8498.99 & -15977.31 \end{bmatrix}$$

$$A_2 = \begin{bmatrix} -2805.96 & -763.30 & 1554.89 \\ -1266.69 & -3005.82 & 1978.34 \\ 1261.52 & 1217.91 & -5060.74 \end{bmatrix} \tag{A2}$$

$$A_3 = \begin{bmatrix} -90.01 & -81.70 & 66.36 \\ -477.65 & -722.58 & 281.67 \\ 25.19 & -10.05 & -37.16 \end{bmatrix}$$

$$A_4 = \begin{bmatrix} 13887.78 & 8605.01 & -20329.47 \\ 10067.41 & 10532.87 & -18437.83 \\ -20113.66 & -13183.07 & 32900.46 \end{bmatrix}$$

Acknowledgments

This research was funded by NASA Dryden Flight Research Center, M. Brenner serving as the Technical Monitor. The authors would like to thank J. Dugundji, E. Crawley, and C. Lin for their help.

References

[1]Kehoe, M. W., "A Historical Overview of Flight Flutter Testing," *Proceedings of the 80th AGARD Structures and Materials Panel, AGARD-CP-566*, Rotterdam, The Netherlands, 1995, pp. 1.1–1.15.

[2]Cooper, J., "Parameter Estimation Methods for Flight Flutter Testing," *Proceedings of the 80th AGARD Structures and Materials Panel, AGARD-CP-566*, Rotterdam, The Netherlands, 1995, pp. 10.1–10.12.

[3]Lin, C., "Towards Optimal Strain Actuated Aeroelastic Control," Ph.D. Thesis, Dept. of Aeronautics and Astronautics, Massachusetts Inst. of Technology, Cambridge, MA, Feb. 1996.

[4]Gupta, K., Brenner, M., and Voelker, L., "Development of an Integrated Aeroservoelastic Analysis Program and Correlation with Test Data," NASA TP-3120, May 1991.

[5]Hassig, H., "An Approximate True Damping Solution of the Flutter Equation by Determinant Iteration," *Journal of Aircraft*, Vol. 8, No. 11, 1971, pp. 885–889.

[6]Nissim, E., and Gilyard, G. B., "Method for Experimental Determination of Flutter Speed by Parameter Identification," *30th Structures, Structural Dynamics, and Materials Conference*, AIAA, Washington, DC, April 1989, pp. 1427–1441 (AIAA Paper 89-1324, 1989).

[7]Brenner, M., and Lind, R., "Robust Flutter Margins of an F/A-18 Aircraft from Aeroelastic Flight Data," *Journal of Guidance, Control, and Dynamics*, Vol. 20, No. 3, 1997, pp. 597–604.

[8]Feron, E., Brenner, M., Paduano, J., and Turevskiy, A., "Time-Frequency Analysis for the Transfer Function Estimation and Application to Flutter Clearance," *Journal of Guidance, Control, and Dynamics*, Vol. 21, No. 3, 1998, pp. 375–382.

[9]Karpel, M., and Strul, E., "Minimum-State Unsteady Aerodynamic Approximations with Flexible Constraints," *Journal of Aircraft*, Vol. 33, No. 6, 1996, pp. 1190–1196.

[10]Balas, G., Doyle, J., Glover, K., Packard, A., and Smith, R., "μ-Analysis and Synthesis Toolbox," MathWorks, Natick, MA, 1994.

[11]Gill, P. E., Murray, W., and Wright, M., *Practical Optimization*, Academic, London, 1994, pp. 115–125.

[12]Reich, G., VanSchoor, M., Lin, C., and Crawley, E., "An Active Aeroelastic Wing Model for Vibration and Flutter Suppression," *36th Structures, Structural Dynamics, and Materials Conference*, AIAA, Washington, DC, April 1995, pp. 314–324 (AIAA Paper 95-1193, 1995).

Discrete-Time Optimal Guidance

R. Gitizadeh* and I. Yaesh†
Israeli Military Industries,
47100 Ramat-Hasharon, Israel
and
J. Z. Ben-Asher‡
Wales, Ltd., 52521 Ramat-Gan, Israel

I. Introduction

MODERN guidance techniques are based mainly on optimal control theory and on differential games.[1,2] Most problems formulated with these methods are solved for continuous-time systems, whereas discrete-time systems are treated numerically.[3] However, most of the applications require discrete-time realizations. In the present work, the most popular guidance problems will be formulated and analytically solved for discrete-time systems. To this end we will use the linear model of a planar pursuit–evasion conflict, assuming ideal pursuer and evader systems.

We consider an evader maneuvering with a constant acceleration and derive discrete-time versions of the proportional navigation (PN) and augmented proportional navigation (APN) guidance laws. These guidance laws turn out to have the same structure as

Received Feb. 25, 1998; revision received Aug. 2, 1998; accepted for publication Aug. 2, 1998.

*Research Engineer, Department of Control and Simulation, IMI-ASD, P.O. Box 1044-77.

†Head, Department of Control and Simulation, IMI-ASD, P.O. Box 1044-77.

‡System Engineer, Hayetsira 29; currently Associate Professor, Department of Aerospace Engineering, Technion—Israel Institute of Technology, 32000 Haifa, Israel. Senior Member AIAA.